

IIT, BOMBAY

SUPERVISED LEARNING PROJECT
AUTUMN 2014

Nonlinear Dynamics of Hodgkin-Huxley Neurons

Author:

Ankit Mahajan
Roll No. 120100027

Supervisor:

Prof. Punit Parmananda

Signature of the Supervisor: _____

Date: _____

Declaration

I, Ankit Mahajan, understand that plagiarism is defined as any one or the combination of the following:

1. Uncredited verbatim copying of individual sentences, paragraphs or illustrations (such as graphs, diagrams, etc.) from any source, published or unpublished, including the internet.
2. Uncredited improper paraphrasing of pages or paragraphs (changing a few words or phrases, or rearranging the original sentence order)
3. Credited verbatim copying of a major portion of a paper (or thesis chapter) without clear delineation of who did or wrote what. (Source: IEEE, The Institute, Dec. 2004)

I have made sure that all the ideas, expressions, graphs, diagrams, etc., that are not a result of my work, are properly credited. Long phrases or sentences that had to be used verbatim from published literature have been clearly identified using quotation marks. I affirm that no portion of my work can be considered as plagiarism and I take full responsibility if such a complaint occurs. I understand fully well that the guide of the seminar report may not be in a position to check for the possibility of such incidences of plagiarism in this body of work.

Signature: _____

Date: _____

Introduction

The aim of this project was to analyze the celebrated Hodgkin-Huxley model of neuronal activity using the techniques of nonlinear dynamics. The quantitative study of electrically active cells received its principal impetus from the remarkable work of Alan Lloyd Hodgkin and Andrew Huxley, in 1951, on nerve conduction in the squid giant axon. Hodgkin and Huxley used voltage-clamp methods to obtain extensive quantitative experimental results and proposed a system of ordinary differential equations that summarized and organized these data. Both of them, together with Sir John Eccles, received the 1963 Nobel Prize in Physiology or Medicine for their groundbreaking work.

In this report, the dynamics of Hodgkin-Huxley neuron is detailed. First, the electrophysiology of neurons is briefly studied. From this a system of four nonlinear differential equations modeling a space-clamped squid axon is derived. A comprehensive understanding of the dynamics displayed by this system remains elusive till date. Part of the reason behind this is the difficulty in applying analytical techniques to a four-dimensional system. So, a numerical approach is adopted here. The results of numerically simulating the system with constant and periodic current forcing are presented. The “threshold” phenomenon in the occurrence of action potentials (neuronal spiking) and its biological significance is discussed.

The good agreement with experimental data on propagating action potentials is one of the major successes of the Hodgkin-Huxley model. The cable theory for describing the behavior of neurons, which are not space-clamped is presented. This leads to a nonlinear PDE system of four equations. Some results obtained by numerically simulating this system are presented.

(Note: The Matlab functions and scripts used for numerical integration and other analysis could be found here: <http://homepages.iitb.ac.in/~120100027/projects.html#HH>)

Contents

1	Electrophysiology of Neurons	4
1.1	Neurons and Action Potentials	4
1.2	The Membrane Potential	5
1.3	Equivalent Circuit	7
1.4	Voltage-gated Channels	8
1.5	The Hodgkin Huxley Model	9
2	Dynamics of the Hodgkin-Huxley Neuron	11
2.1	Action Potential	11
2.2	Bifurcation Analysis	16
2.3	Resonance	18
2.4	Cable Theory	19

Chapter 1

Electrophysiology of Neurons

In this chapter, we begin with some preliminary information about neurons and their biological functioning. Then we move on to study the electrochemistry of the ions responsible for regulation of membrane potential. An electrical equivalent circuit of the neuron membrane is presented. Finally, based on the equivalent circuit representation the Hodgkin-Huxley system of equations is put forth.

1.1 Neurons and Action Potentials

Neurons are the building blocks of the nervous system. They are electrically excitable cells that transmit information throughout the body in electrical and chemical signals.

Neurons come in many different shapes and sizes. Some of the smallest neurons have cell bodies that are only 4 microns wide. Some of the biggest neurons have cell bodies that are 100 microns wide. A typical neuron is divided into three parts: the soma or cell body, dendrites, and axon. The soma is usually compact; the axon and dendrites are filaments that extrude from it. Dendrites typically branch profusely and extend their farthest branches a few hundred micrometers from the soma. The axon leaves the soma at a swelling called the axon hillock, and can extend for great distances, giving rise to hundreds of branches. The squid giant axon, used by Hodgkin and Huxley in their experiments, is the very large axon (up to 1 mm in diameter; typically around 0.5 mm) that controls part of the water jet propulsion system in squid.

Synaptic signals from other neurons are received by the soma and dendrites; signals to other neurons are transmitted by the axon. Synapse is a contact between the axon of one neuron and a dendrite or soma of another.

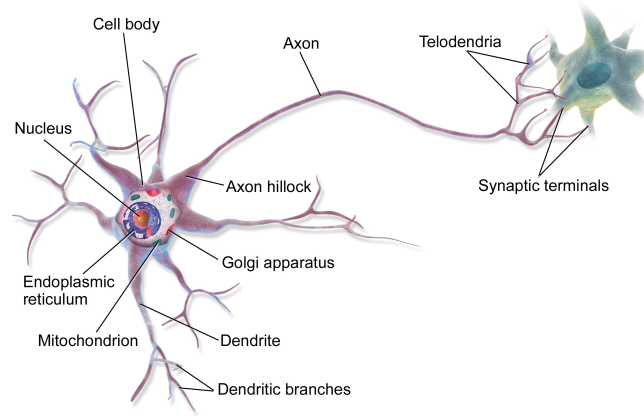


Figure 1.1: A typical neuron (Source: Wikipedia)

In a chemical synapse, electrical activity in the presynaptic neuron is converted (via the activation of voltage-gated calcium channels) into the release of a chemical called a neurotransmitter that binds to receptors located in the plasma membrane of the postsynaptic cell. The neurotransmitter may initiate an electrical response, called postsynaptic potentials (PSPs), or a secondary messenger pathway that may either excite or inhibit the postsynaptic neuron. In an electrical synapse, the presynaptic and postsynaptic cell membranes are connected by special channels called gap junctions that are capable of passing electric current, causing voltage changes in the presynaptic cell to induce voltage changes in the postsynaptic cell. A typical neuron receives inputs from more than 10,000 other neurons through synapses; see fig. (1.1). Small currents produce small PSPs; larger currents produce significant PSPs that can be amplified by the voltage-sensitive channels embedded in the neuronal membrane and lead to the generation of an action potential or spike—an abrupt and transient change of membrane voltage that propagates to other neurons via the axon. Such spikes are the main means of communication between neurons.

1.2 The Membrane Potential

All living cells have a potential difference between their inside and outside, referred to as the membrane potential.

$$V_m = V_{in} - V_{out}$$

The resting potential refers to the potential across the membrane when the cell is at rest. A typical neuron has a resting potential of about -70mV.

The potential difference arises from differences in the concentrations of ions within and outside the cell. The maintenance of the potential difference involves the transport of ions across the cell membrane and the selective permeability of the membrane to these ions. Most of these transmembrane currents involve one of three ionic species: sodium (Na^+), potassium (K^+), or chloride (Cl^-). The concentration of K^+ ions inside a cell is about 10 times that in the extracellular fluid, whereas the concentrations of Na^+ and Cl^- are much higher outside the cell than inside.

The lipid bilayer of the cell membrane is a poor conductor of ionic current because it is not permeable to ions. However, the membrane does contain channel proteins that allow for the ions to move through it. There are two types of ion channels in the membrane: gated and nongated. Nongated channels are always open, whereas gated channels can open and close and the probability of opening often depends on the membrane potential; these are referred to as voltage-gated channels. Gated channels are typically selective for a single ion. The permeability of the membrane to a particular ion depends on the number of open channels selective for that ion. Most gated channels are closed at rest; hence, the nongated ion channels are primarily responsible for establishing the resting potential. An action potential is generated when gated channels open allowing for the flux of ions across the cell membrane. There are two forces that drive each ion species through the membrane channel: concentration and electric potential gradients. Because of concentration differences, when the appropriate channels are open, Na^+ and Cl^- ions tend to diffuse into the cell, whereas K^+ ions tend to diffuse outward. This sets up an electric potential gradient across the membrane. Interplay between these two counteracting forces results in a constant resting potential. It depends on the concentrations of the ions both inside and outside the cell, as well as the permeability of the cell membrane to each of the ions.

For a cell to maintain a constant resting potential, the efflux of K^+ ions must balance the influx of Na^+ ions (here we are ignoring Cl^- ions). That is, the charge separation across the membrane must be constant. If these steady ion leaks continued unopposed, then K^+ ions within the cell would become depleted, whereas the concentration of Na^+ ions inside the cell would increase. This would eventually result in a loss of the ionic gradients, necessary for maintaining the resting potential. The dissipation of ionic gradients is prevented by active pumps that extrude Na^+ ions from the cell while taking in K^+ . The Na^+K^+ pump is an integral membrane protein that exchanges three Na^+ ions for two K^+ ions.

The Nernst potential of an ion is given by,

$$E_{ion} = \frac{RT}{zF} \ln \frac{[Ion]_{out}}{[Ion]_{in}} \quad (1.1)$$

where $[Ion]_{in}$ and $[Ion]_{out}$ are concentrations of the ions inside and outside the cell, respectively; R is the universal gas constant (8,315 mJ/(KMol)); T is temperature; F is Faradays constant (96,480 coulombs/Mol) and z is the valence of the ion. Suppose the membrane is only permeable to K^+ ions. Then, the K^+ Nernst potential is the potential at which K^+ ions are in equilibrium across the membrane. This potential is also called the reversal or equilibrium potential of the K^+ ion.

Neurons at rest are permeable to Na^+ and Cl^- in addition to K^+ . Because of their concentration differences, Na^+ and Cl^- ions move into the cell and K^+ ions move outward. The influx of Na^+ ions tends to depolarize the cell, whereas the efflux of K^+ and the influx of Cl^- have the opposite effect. The resting potential of the cell is the potential at which there is a balance between these fluxes. Thus the resting potential is a steady state rather than an equilibrium state, as there are nonzero ion fluxes. An expression for resting potential is given by the GoldmanHodgkinKatz(GHK) equation,

$$V_m = \frac{RT}{F} \ln \frac{P_K[K^+]_{out} + P_{Na}[Na^+]_{out} + P_{Cl}[Cl^-]_{in}}{P_K[K^+]_{in} + P_{Na}[Na^+]_{in} + P_{Cl}[Cl^-]_{out}} \quad (1.2)$$

where P_{ion} is the permeability of the membrane to the ion [8]. Although the GHK equation gives an accurate description of the membrane potential, it will not be used in the analysis that follows. Instead a more amenable equivalent electrical circuit description (described in the next section) will be used.

1.3 Equivalent Circuit

In the equivalent circuit, ion channels are represented as a conductor in series with a battery. When the membrane potential equals the Nernst potential, say E_{ion} , the net ion current, denoted as i_{ion} (A/cm²), is zero [4, 8]. Otherwise, the net ion current is proportional to the difference of potentials; that is,

$$i_{ion} = g_{ion}(V_m - E_{ion}) \quad (1.3)$$

where g_{ion} (mS/cm²) is the specific membrane conductance and $(V - E_{ion})$ is the ion driving force. The electrical properties of the squid axon rely primarily on K^+ and Na^+ ions. Thus the net ion current is given by,

$$i_{ion} = g_K(V_m - E_K) + g_{Na}(V_m - E_{Na}) + g_L(V_m - E_L) \quad (1.4)$$

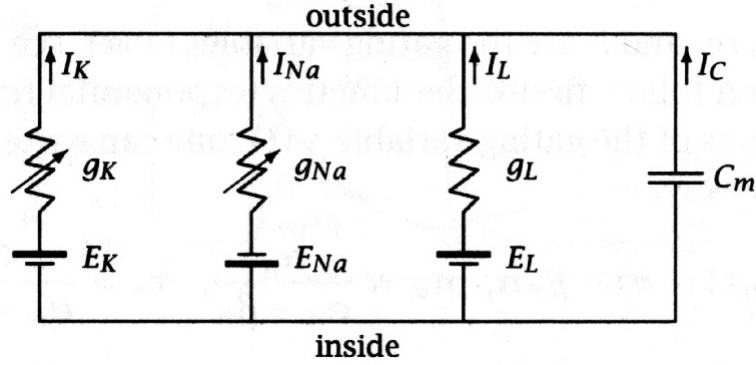


Figure 1.2: The equivalent circuit of the squid axon

where the last term represents the leaky current i.e. the current through nongated ion channels.

The lipid bilayer that constitutes the cell membrane has dielectric properties and as such behaves in much the same manner as a capacitor. Thus the bilayer is represented by a capacitor with specific membrane capacitance c_m in the equivalent circuit.

$$i_{cap} = c_m \frac{dV_m}{dt} \quad (1.5)$$

1.4 Voltage-gated Channels

In the HodgkinHuxley model, each channel is viewed as a transmembrane protein that forms a pore through which ions can diffuse down their concentration gradients. The pores have gates that can be either open or closed; the probability that a gate is open or closed may depend on the membrane potential, Intracellular agents (second-messengers) or Extracellular agents (neurotransmitters and neuromodulators). When the gating particles are sensitive to the membrane potential, the channels are said to be voltage-gated.

$$C \xrightleftharpoons[\beta(V)]{\alpha(V)} O \quad (1.6)$$

where C and O correspond to the closed and open states, respectively, and $\alpha(V)$ and $\beta(V)$ are the voltage-dependent rate constants at which a gate goes from the closed to the open and from the open to the closed states, respectively. If we let m be the fraction of open gates, then $1 - m$ is the

fraction of closed gates, and, from the law of mass action,

$$\frac{dm}{dt} = \alpha(V)(1 - m) - \beta(V)m = \frac{m_{\infty(V)} - m}{\tau(V)} \quad (1.7)$$

where,

$$m_{\infty(V)} = \frac{\alpha(V)}{\alpha(V) + \beta(V)}, \quad \tau(V) = \frac{1}{\alpha(V) + \beta(V)}$$

The gates are divided into two types: those that activate or open the channels, and those that inactivate or close them. The probability of an activation gate being in the open state is denoted by the variable m for Na^+ and n for K^+ . The probability of an inactivation gate being in the open state is denoted by the variable h . The proportion of open Na^+ channels in a large population is

$$p = m^a h^b$$

where a is the number of activation gates and b is the number of inactivation gates per channel [4].

Based on the experimentally measured conductances of isolated ion currents at a fixed voltage (voltage-clamp), Hodgkin and Huxley proposed,

$$g_K = \bar{g}_K n^4, \quad g_{Na} = \bar{g}_{Na} m^3 h \quad (1.8)$$

where \bar{g}_K and \bar{g}_{Na} are maximum conductances. Each of the gating variables satisfy the time evolution equation of the form (1.7). They also chose the rate functions $\alpha(V)$ and $\beta(V)$ to fit the voltage-clamp experiment data.

1.5 The Hodgkin Huxley Model

In this section we put it all together and obtain a nonlinear system of differential equations. An additional space-clamp condition has been assumed throughout; longitudinal currents are eliminated by the use of internal axial and external guard electrodes, and the state of the membrane is always spatially uniform. In the equivalent circuit, by charge conservation,

$$i = i_{ion} + i_{cap} \quad (1.9)$$

Thus using equations (1.4), (1.5) and (1.8), we get,

$$c_m \dot{V} = i - \bar{g}_K n^4 (V - E_K) - \bar{g}_{Na} m^3 h (V - E_{Na}) - g_L (V - E_L) \quad (1.10a)$$

$$\dot{m} = \alpha_m(V)(1 - m) - \beta_m(V)m \quad (1.10b)$$

$$\dot{n} = \alpha_n(V)(1 - n) - \beta_n(V)n \quad (1.10c)$$

$$\dot{h} = \alpha_h(V)(1 - h) - \beta_h(V)h \quad (1.10d)$$

where,

$$\begin{aligned}\alpha_n(V) &= 0.01 \frac{10 - V}{\exp(\frac{10-V}{10}) - 1} \\ \beta_n(V) &= 0.125 \exp(-\frac{V}{80}) \\ \alpha_m(V) &= 0.1 \frac{25 - V}{\exp(\frac{25-V}{10}) - 1} \\ \beta_m(V) &= 4 \exp(-\frac{V}{18}) \\ \alpha_h(V) &= 0.07 \exp(-\frac{V}{20}) \\ \beta_h(V) &= \frac{1}{\exp(\frac{30-V}{10}) + 1}\end{aligned}$$

$$\begin{aligned}E_K &= -12mV, & E_{Na} &= 115mV, & E_L &= 10.6mV \\ \bar{g}_K &= 36mS/cm^2, & \bar{g}_{Na} &= 120mS/cm^2, & \bar{g}_L &= 0.3mS/cm^2, & c_m &= 1\mu F/cm^2\end{aligned}$$

Note: These are the equations used in the original HH papers. Here the resting potential is shifted to 0mV (the actual value is $-65mV$) [1].

Although the Hodgkin-Huxley equations were originally based on experimental voltage-clamp data, it was found that when they were solved under current-clamp conditions, the important physiological properties of excitation were reproduced. The effect of temperature on the gating variable dynamics is also ignored.¹

¹We assume that the temperature is fixed at $6.3^\circ C$

Chapter 2

Dynamics of the Hodgkin-Huxley Neuron

In this chapter, solutions of the HH system of equations (1.10) are discussed. The action potential response of the HH neuron is analyzed. The subtle concept of “threshold” is discussed. Bifurcation analysis of the system is done with constant external current as the parameter. Finally, the space-clamp condition is lifted and the cable equation is derived.

2.1 Action Potential

A mathematically rigorous linear stability analysis of the HH system is rather difficult because of the high dimensionality of the system. The traditional approach to get around this is to reduce the dimensionality of the system, by ignoring the dynamics of the variables with large time constants [2, 3]. In this section a vivid albeit heuristic picture of the dynamics is presented to get some insight into the action potential response of the HH neuron.

2.1.1 The V-m reduced system

The following plots of the steady values and time constants (1.7) of gating variables against the membrane voltage provide a qualitative description of their dynamics. The times constants of variables n and h are much bigger than that of m ; n and h change their values more slowly than m . Thus we (temporarily) ignore the dynamics of n and h in the HH equations and

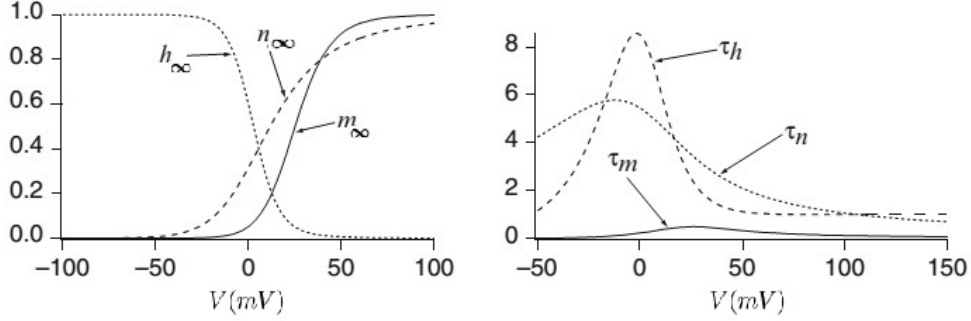


Figure 2.1: The steady state values and time constants of gating variables

consider the V-m subsystem:

$$c_m \dot{V} = i - \bar{g}_K n^4 (V - E_K) - \bar{g}_{Na} m^3 h (V - E_{Na}) - g_L (V - E_L) \quad (2.1a)$$

$$\dot{m} = \alpha_m(V)(1 - m) - \beta_m(V)m \quad (2.1b)$$

$$(2.1c)$$

h , n and i are treated as parameters. The equations of the nullclines obtained by equating \dot{V} and \dot{m} to zero are,

$$\text{V nullcline:} \quad m = \left[\frac{i - \bar{g}_K n^4 (V - E_K) - g_L (V - E_L)}{\bar{g}_{Na} h (V - E_{Na})} \right]^{1/3} \quad (2.2)$$

$$\text{m nullcline:} \quad m = \frac{\alpha_m(V)}{\alpha_m(V) + \beta_m(V)} = m_\infty(V) \quad (2.3)$$

The nullclines for both the variables are shown in fig. (2.2) for $i = 0$, $n = 0.31$ and $h = 0.59$.

The two nullclines intersect each other at three singular points (equilibrium or steady-state points). v_1^* and v_3^* are stable nodes, while v_2^* is a saddle point.¹ The stable separatrix, which can be called threshold separatrix, forms a boundary in the phase plane at which a threshold phenomenon occurs. The region on the left of this separatrix is the basin of attraction of v_1^* , while that on the right side is the basin of attraction of v_3^* . An instantaneous current pulse (ideally a delta function) at $t = 0$ will displace the phase point of the resting system horizontally to the right from v_1^* . If the stimulus is strong enough, the displaced phase point will end up on the right side of the threshold separatrix, thus will be attracted towards v_3^* . The action potential for

¹Eigenvalues of the jacobian of the coefficient matrix at these points are, v_1^* : $(-0.25, -4.62)$, v_2^* : $(0.24, -4.60)$, v_3^* : $(-9.51, -71.43)$

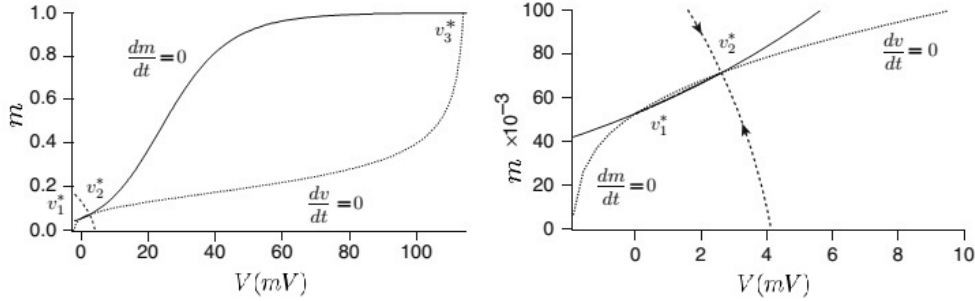


Figure 2.2: The V and m nullclines (the second subfigure is the magnified view of the first)

this reduced system, with h and n at their resting values, shows a rising phase similar to that of a real nerve, followed by a permanent plateau. This system therefore shows no recovery to the resting state, for which changes in h and n need to be considered.

Let's consider the effects of changing the values of n , h and i on V and m nullclines. As can be seen from equation (2.3), the m nullcline is unaffected by changes in these parameters. According to equation (2.2), for any fixed V , m is increased by a positive change of i or of n , or by a negative change of h . These changes therefore raise the V nullcline, although not uniformly over the whole V axis. The V nullcline is lowered by opposite changes of i , n , or h .

Now let analyze the effects of changing h and n on the dynamics. At any instant, the phase point will be moving in time along some path of the V - m phase plane corresponding to the value of h and n at that instant. It should be pointed out that the idea of a phase point moving along paths which are themselves moving about in a phase plane is not mathematically rigorous and is only used as an aid to the imagination. As the neuron becomes depolarized due to the impulse, the value of h_∞ decreases and that of n_∞ increases. As h and n tend slowly towards these values the V nullcline shifts upward and points v_2^* and v_3^* move towards each other eventually annihilating each other (fig. (2.3)). Now v_1^* is the only attractor in the phase plane and the phase point retreats towards this node. From here on, the phase point remains nearly at the slowly moving stable singular point v_1^* . Since V is now negative, \dot{h} and \dot{n} reverse sign, h and n approach new resting values, the V nullcline falls again, and v_1^* returns slowly to its original resting position. The time interval during which v_2^* is absent is the absolute refractory period. When v_2^* finally returns, it is far away from v_1^* (where the phase point now is,

approximately), and therefore the threshold value of V necessary for a second excitation is larger than in the resting state. As long as this is true, the system is relatively refractory. This is the mathematical basis of refractoriness in the H-H equations.

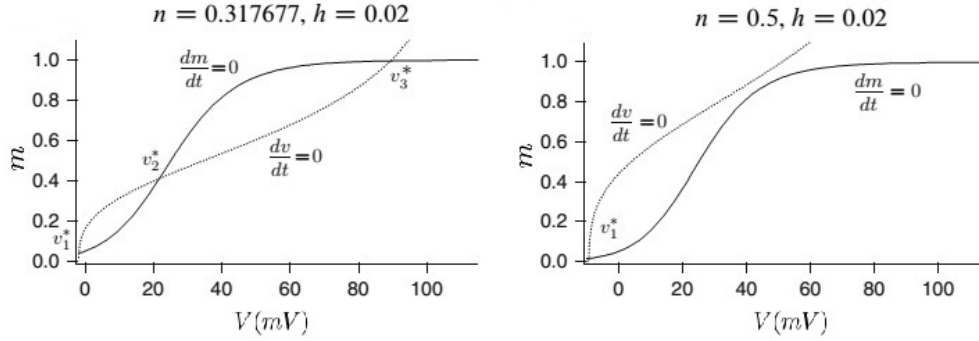


Figure 2.3: Effect of change in the values of h and n on the V nullcline

The entire (V, m, h, n) phase space can be examined for the presence of singular points. In fig. (2.4) is plotted the V, h, n nullcline as a dashed curve, representing the projection onto the (V, m) plane of the curve of intersection of the three nullclinal three-dimensional hypersurfaces for V, h , and n in the (V, m, h, n) space. This curve intersects the m nullcline only at $V = 0$, so that in the V, m, h, n system there is only one singular point A.

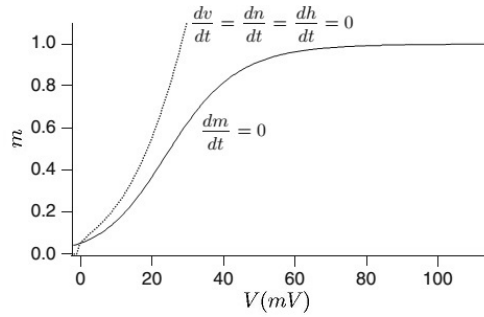


Figure 2.4: The equilibrium point of the full system

The fact that the complete equations have no saddle point made it difficult to understand why they had such a sharp threshold. This sharp threshold can now be explained by the saddle point B which does exist for h and n near their resting values in the V, m reduced system. The system is said to exhibit a “quasi threshold phenomenon” (QTP). In a QTP, there is no saddle

point in the complete system, and any intermediate response between “all” and “none” is obtainable by an accurate enough adjustment of the stimulus intensity.

2.1.2 Physiology of an Action Potential

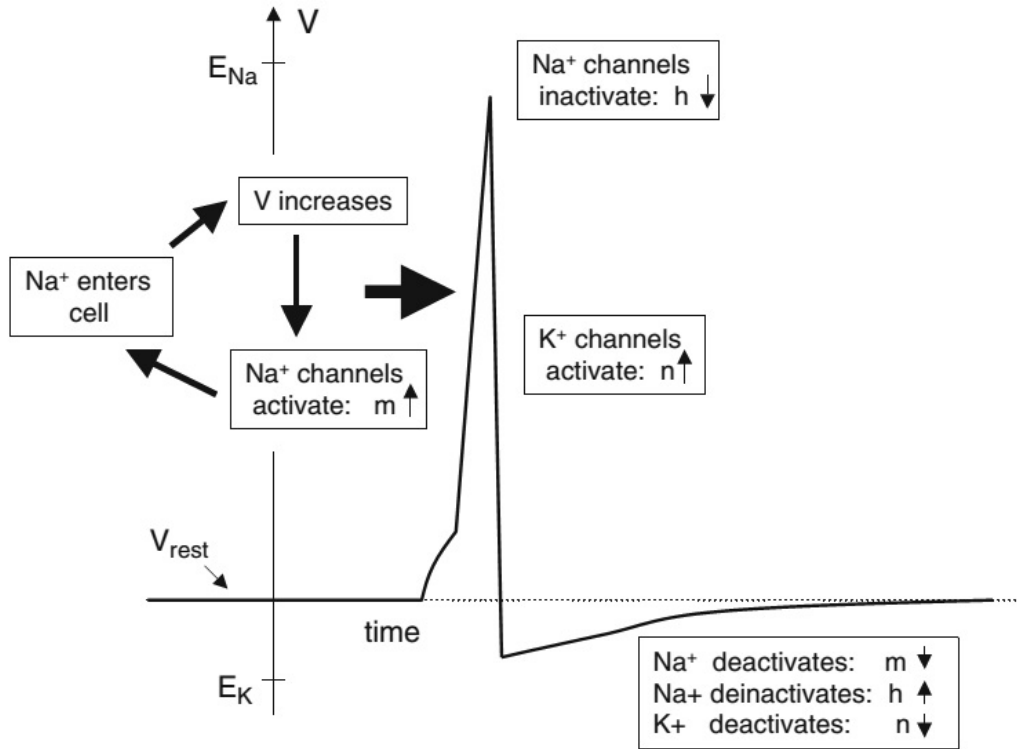


Figure 2.5: Action Potential [8]

When the neuron is depolarized due to the stimulus, values of the activation curves are changed: m_∞ and n_∞ increase, whereas h_∞ decreases. Since n , m , and h tend toward their activation curves, it follows that n and m initially increase, whereas h decreases. That is, K^+ channels open, whereas Na^+ channels both activate and inactivate. However, m is much smaller than both n and h . It follows that the Na^+ channels activate much faster than they inactivate or K^+ channels open. Therefore, the Na^+ conductance, increases faster than that of K^+ . The increase in the Na^+ conductance leads to a large increase in the Na^+ current. As long as the neuron is near rest, the driving force $V - E_{Na}$ is large. Hence, the Na^+ current will dominate the equation for the membrane potential and V will increase toward the Na^+ Nernst po-

tential. As V increases, m_∞ increases further, leading to further increase in Na^+ activation. As V increases toward E_{Na} , Na^+ channels inactivate. This is because h tends to h_∞ which is close to zero. Moreover, the Na^+ driving force $V - E_{\text{Na}}$ decreases. For both reasons, the Na^+ current turns off. Meanwhile, the K^+ channel activates because n tends to m_∞ which is almost one. Moreover, the K^+ driving force $V - E_K$ becomes very large. It follows that eventually, the K^+ current dominates and the membrane potential must fall back toward the K^+ Nernst potential. This corresponds to the downstroke of the action potential. After the action potential, the cell is hyperpolarized. After some time, m , n and h approach their steady-state values and the cell returns to rest.

2.2 Bifurcation Analysis

In this section the bifurcation analysis of the HH neuron with constant current clamp is done with the current(i) as the parameter [6]. The neuron model produces an action potential in response to an external pulsatile stimulus. We can expect that the neuron generates action potentials persistently when a continuous current is applied externally.

The Jacobian matrix corresponding to Equations (1.10), tedious to derive by hand, is found easily in Matlab. All the results below were verified using the Jacobian and numerical integration of the system.

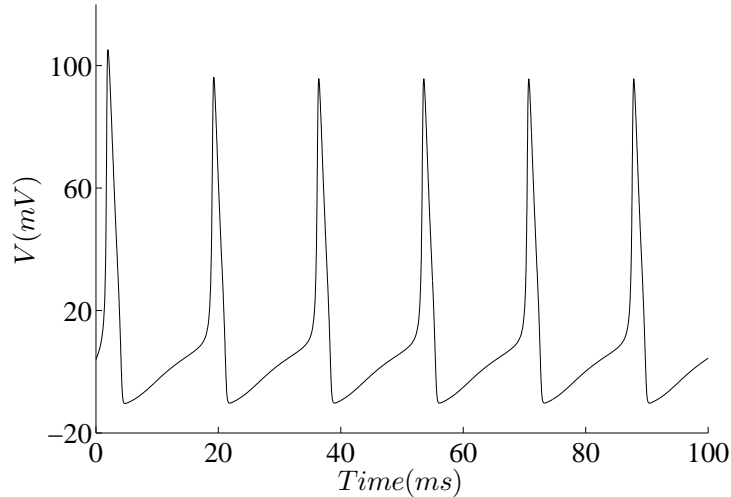


Figure 2.6: V time series for $i = 7\mu\text{A}/\text{cm}^2$ and resting state as the initial state

For all values of i there is a single fixed point. For $0 < i < 6.3\mu\text{A}/\text{cm}^2$,

the fixed point is a stable focus. For $6.3\mu A/cm^2 < I < 9.8\mu A/cm^2$, starting from the resting state, persistent chain of action potentials results (fig. 2.6).

At $t = 62ms$, a pulsatile stimulus is applied to the neuron in addition to the constant current injection. After the pulse stimulus, the repetitive firing is stopped in spite of the persistent injection of the constant current. This means that an repetitive firing (stable limit cycle) and a quiescent state (stable equilibrium) coexist when $i = 7$. The state point of the HH neuron is moved from limit cycle to the basin of attraction of the stable focus. The boundary between the two basins of attraction is an unstable limit cycle.(fig. (2.7))

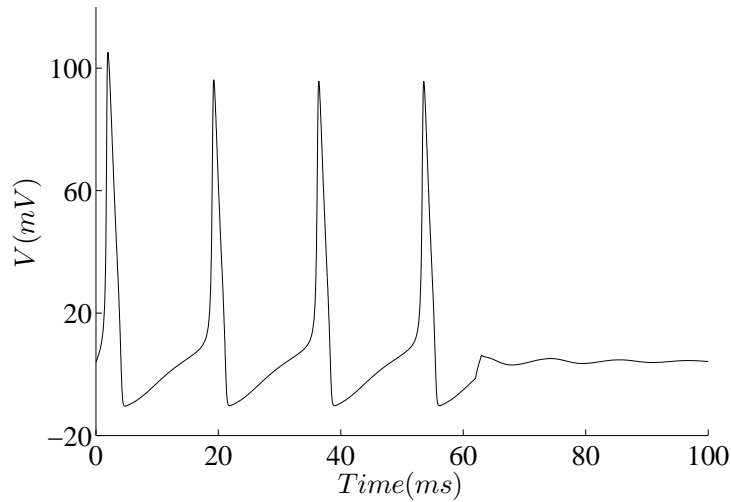


Figure 2.7: Hysteresis

Fig. (2.8) shows the dependence of the solution of the HH equations on the parameter i ; the V values of the stationary solution of the HH equations are plotted for various values of i where the maximum and minimum values of V are plotted for a periodic (oscillatory) solution. Solid and dotted curves denote stable and unstable equilibria, respectively. The filled (open) circles denote stable (unstable, resp.) periodic solutions.

At $i = 6.3\mu A/cm^2$, a double-cycle bifurcation or saddle-node bifurcation of periodics occurs and a pair of stable and unstable periodic solutions is generated. An unstable periodic solution is bifurcated by the sub-critical Hopf bifurcation at $i = 9.8\mu A/cm^2$.²

²Near $i = 7.9\mu A/cm^2$, four periodic solutions (one stable solution and three unstable solutions) coexist as a result of double-cycle bifurcation. These occur in a narrow range of parameter values and are hard to locate numerically. In this region period doubling bifurcations of unstable limit cycles are also observed. Chaotic solutions have been hy-

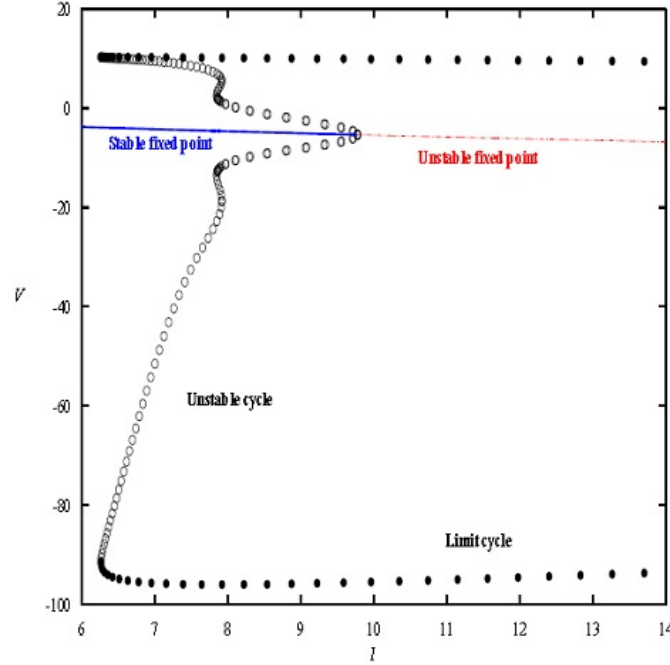


Figure 2.8: Bifurcation diagram [9]

2.3 Resonance

It was observed in the last section that, a HH neuron is an autonomous self-sustained oscillator. Thus from the nonlinear interaction between the frequencies of the system and the stimulus, neurons under periodic stimulus exhibit rich dynamical responses including mode locking, quasiperiodicity and chaos. All these phenomena have been observed experimentally in the giant squid axon [7].

Fig. (??) shows the damped dynamics of an unperturbed neuron. Note that the fourier transform peaks at around 54 Hz(ν_0). The periodic stimulus is modeled as $i = I_0 \cos(2\pi\nu t)$ in (1.10). It is found by numerical integration that for each perturbation frequency (ν), for the stimulus to elicit persistent action potential response the amplitude I_0 has to be above a threshold value, which itself is a function of ν . Plotting these threshold amplitudes against forcing frequency gives a U-shaped curve called the “Arnold tongue” (fig. ??). Note that the minimum of the dotted curve denoting the bound-

pothesized to occur through period-doubling route in an even narrower parameter range [5].

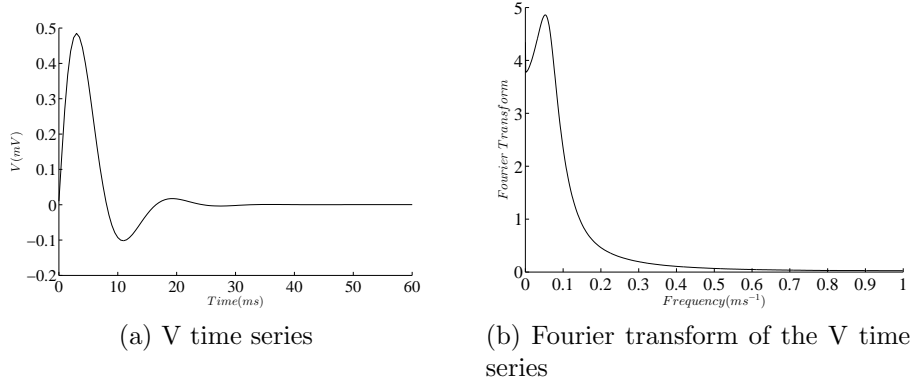


Figure 2.9: Unperturbed HH neuron

ary of non-firing region occurs at a frequency approximately equal to ν_0 , thus confirming the resonance phenomenon in the system [10]. For values of forcing parameters inside this curve, frequency entrainment is observed.

Fig. (2.11) illustrates the phenomenon of phase locking. The system has been shown to exhibit chaotic dynamics arising from the intermittency route to chaos [7].

2.4 Cable Theory

In this section the HH model is modified by relaxing the space-clamp constraint. This leads to a four dimensional nonlinear PDE system, which is used to explain the wave propagation phenomena in neurons. First a brief account of passive cable theory and its limitations is given. Then the HH cable theory is developed and some solutions obtained by numerical integration are presented.

2.4.1 Passive Cable Theory

Consider a cell that is shaped as a long cylinder, or cable, of radius a . We assume the current flow is along a single spatial dimension, x , the distance along the cable. In particular, the membrane potential depends only on the x variable, not on the radial or angular components. The membrane is modeled as a leaky capacitor (capacitance per unit length c_m) whose resistance (resistance times unit length r_m) is independent of the membrane voltage. It is assumed that axoplasm behaves like a linear, Ohmic conductor whose resistance per unit length is r_i . The extracellular fluid is isopotential and

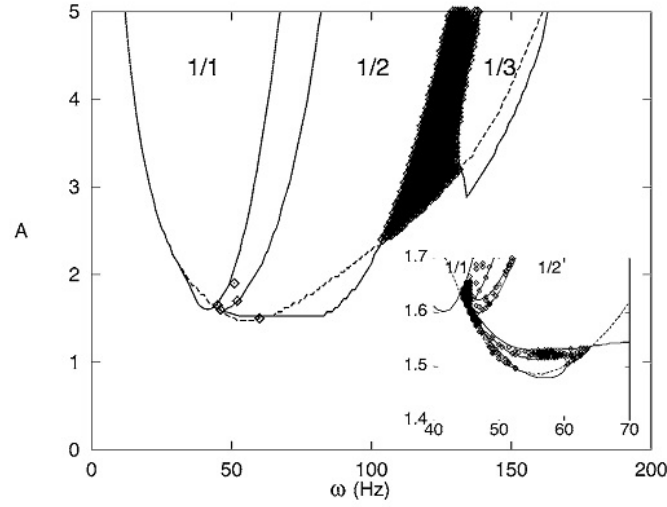


Figure 2.10: Phase diagram of the Hodgkin-Huxley neuron under sinusoidal stimuli in the parameter space of the forcing amplitude A and frequency ω . The phase boundaries of $1/1$, $1/2$ and $1/3$ mode locked states are represented by solid curves and those of non-firing state by dotted curves. The chaotic states with positive Lyapunov exponent are denoted as diamonds. Inset: the detailed phase diagram near $\omega = 50\text{Hz}$ and $A = 1.5\mu\text{A}/\text{cm}^2$ [11]

resistanceless. The equivalent circuit is shown in fig. (2.12).

Applying Ohm's law along the axis,

$$r_i I_i = -\pi a^2 \frac{\partial V}{\partial x} \quad (2.4)$$

Matching potentials across the membrane,

$$i_m = c_m \frac{\partial V}{\partial x} + \frac{V}{r_m} \quad (2.5)$$

The membrane current is given by current conservation,

$$i_m = -\frac{\partial I_i}{\partial x} \quad (2.6)$$

These three equations can be combined to yield the passive cable equation,

$$\lambda^2 \frac{\partial^2 V}{\partial x^2} = V + \tau \frac{\partial V}{\partial t} \quad (2.7)$$

where, $\lambda = \sqrt{ar_m/2r_i}$ and $\tau = c_m r_m$.

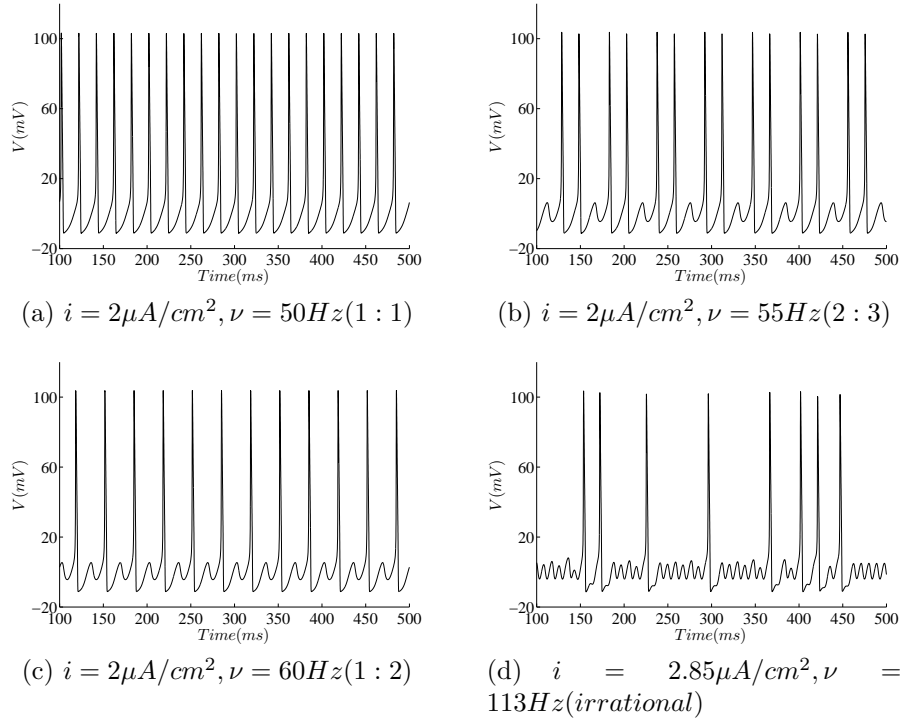


Figure 2.11: Phase locking

Let's consider the steady state solutions of this PDE. Consider a semi-infinite cable (defined for $x > 0$) in which a step of current, I_0 is injected at $x = 0$. As $t \rightarrow \infty$, the solution $V(x, t)$ approaches a steady-state solution $V_s(x)$. Setting $\partial V / \partial t = 0$ in equation (2.7),

$$\lambda^2 \frac{d^2 V_s}{dx^2} - V_s = 0 \quad (2.8)$$

The boundary condition is,

$$r_i I_0 = -\frac{dV_s}{dx}(0) \quad (2.9)$$

The solution is given by,

$$V_s(x) = -\frac{\lambda r_i}{\pi a^2} I_0 e^{(-x/\lambda)} \quad (2.10)$$

Thus the potential decays exponentially with distance from the stimulus. But real neuron needs to and does communicate signals over large distances with very little attenuation[8]. This caveat is resolved by modeling the membrane as a cable of HH circuit units.

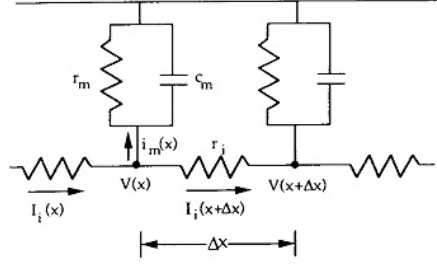


Figure 2.12: Equivalent circuit of a passive cable

2.4.2 Active Cable Theory

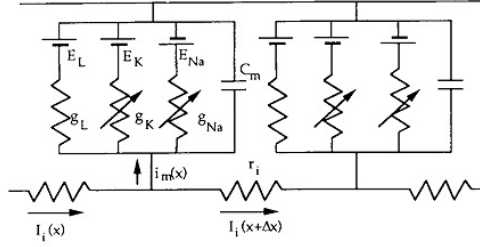


Figure 2.13: Equivalent circuit of an active cable

To implement the Hodgkin-Huxley model, the passive cable model is modified as shown in fig. (2.13). Here the membrane resistance times unit length r_m , is replaced by an active model of the voltage dependent sodium, potassium, and leakage channels. With these modifications the membrane current equation (2.5) is modified to,

$$i_m = c_m \frac{\partial V}{\partial t} + i_K + i_{Na} + i_L \quad (2.11)$$

Thus the following system of equations is obtained,

$$c_m \frac{\partial V}{\partial t} = \frac{a}{2r_i} \frac{\partial^2 V}{\partial x^2} - \bar{g}_K n^4 (V - E_K) - \bar{g}_{Na} m^3 h (V - E_{Na}) - g_L (V - E_L) \quad (2.12a)$$

$$\frac{\partial m}{\partial t} = \alpha_m(V)(1 - m) - \beta_m(V)m \quad (2.12b)$$

$$\frac{\partial n}{\partial t} = \alpha_n(V)(1 - n) - \beta_n(V)n \quad (2.12c)$$

$$\frac{\partial h}{\partial t} = \alpha_h(V)(1 - h) - \beta_h(V)h \quad (2.12d)$$

These equations constitute a system of four, nonlinear, coupled PDEs. They are solved numerically for the transmembrane potential $V(x, t)$ and the three gating parameters $m(x, t)$, $n(x, t)$, and $h(x, t)$, using the method of lines. Hodgkin and Huxley were able to show that the propagation velocity $u \propto \sqrt{a}$, in good agreement with measurements in real neurons. The propagating action potential has the correct shape and amplitude. The computed propagation velocity of $u = 18.8m/s$, is very close to the experimental value of $21.2m/s$ [1].

Bibliography

- [1] A. L. Hodgkin, and A. F. Huxley, 1952, A quantitative description of membrane current and its application to conduction and excitation in nerve, *J. Physiol.*, 117, 500.
- [2] R. FitzHugh, 1960, Thresholds and plateaus in the Hodgkin-Huxley nerve equations, *J. Gen. Physiol.*, 43, 867.
- [3] R. FitzHugh, 1961, Impulses and physiological states in theoretical models of nerve membrane. *Biophysical J.* 1:445-466
- [4] E. M. Izhikevich, 2007, *Dynamical Systems in Neuroscience: The Geometry of Excitability and Bursting*, The MIT press
- [5] J. Guckenheimer, and Ricardo A. Oliva, 2002, *SIAM J. Applied Dynamical Systems*, Vol. 1, No. 1, pp. 105-114
- [6] J. Rinzel and R. Miller, 1980, Numerical calculation of stable and unstable periodic solutions to the Hodgkin-Huxley equations, *Math. Biosci.*, 49, pp. 27-59
- [7] K. Aihara and G. Matsumoto, 1986, Chaotic oscillations and bifurcations in squid giant axons, in *Chaos*, A. Holden, ed., Manchester University Press, Manchester, UK, pp. 257-269.
- [8] G. B. Ermentrout, and David H. Terman, 2010, *Mathematical Foundations of Neuroscience*, Springer Science and Business Media
- [9] K. K. Lin, 2005, Entrainment and chaos in a pulse-driven Hodgkin-Huxley oscillator, *arXiv:math/0505161 [math.DS]*
- [10] P. Parmananda, Claudia H. Mena, and Gerold Baier, 2002, Resonant forcing of a silent Hodgkin-Huxley neuron, *Physical Review E* 66, 047202

- [11] S. Lee and S. Kim, 2006, Bifurcation analysis of mode-locking structure in a Hodgkin-Huxley neuron under sinusoidal current, *Physical Review E* 73, 041924